where $\sigma^2_{v_i} = \left\langle [v_i(t)]^2 \right\rangle_t - \left[\langle v_i(t) \rangle_t \right]^2$.

The value of $\chi(N)$ provides us the degree of the network synchronization. The unitary synchronization value corresponds to a totally synchronous system and the null one to a complete asynchronous one.

As argued in Chapter 1, a FitzHugh-Nagumo modelled cell experiences different states when an input perturbs its quiescent state. Thus, the χ-measure takes into account the in-phase synchronization concerning all the states, not only the excited one. This means that, for example, in the trivial case of all the cells in the quiescent state for all the time, the system results totally synchronized, i.e., $\chi(N) = 1$. It follows that networks with low activity have an high synchronization level, as we will specify later on.

Several aspects influence the network synchronization degree. Apart from the intrinsic characteristics of neurons, network connectivity properties are also an important aspect. For example, the authors in [36] provide synchronization values as a function of the connectivity parameter of the small-world networks, as well as of the connectivity strength g_{syn}. Inspired by the treatment in [36], we consider here three different cases: two of them involve differences in the topology while the third one introduces the presence of two kinds of neurons, the excitatory and the inhibitory ones. We present them in order to show several examples of dynamics and to provide their synchronization value.

Simulations are done by exploiting a domain triangular decomposition of the domain, which is borrowed from the FEM technique. All technicalities are specified in the previous chapter or can be found in [6]. In all solutions presented below, a null initial datum is considered on the whole domain. A non-trivial dynamics is performed by a continuous current injected to several neurons. In particular, we consider a population of 7933 neurons standing on a triangular mesh over the domain $B = [0, 1]^2$; 318 of them receive a continuous current $I = 0.1$. Focusing on a single neuron which receives this current, it is worth noting that it joins a stable limit cycle (this follows by Chapter 1). The parameters considered in simulations are the following:

$$g_{\text{syn}} = 0.01, \quad d = 0.01, \quad v^E_{\text{syn}} = 0.93, \quad v_T = 0.9, \quad R_i = 1/16 \ \forall i, \ , \tag{4.8}$$

while the v^I_{syn} value will be specified later on.

4.2.1 Quasi-regular topology

In this first case, we define the topology as follows. Each neuron is supposed to get electrical inputs through gap junctions from its nearest-neighbours as described in (2.28). Chemical synapses exist between one neuron and those laying on a circle having a fixed radius. In order to introduce a certain heterogeneity degree, we suppose that not all synapses are active: the 25% of them randomly chosen are switched off. The probability of the turning off of connections is supposed to be uniformly distributed. This ensures, as grounded on experimental evidences, that not all chemical synapses are bidirectional. The dynamics is shown in Figures 4.3-4.4-4.5. In particular, Figure 4.3 depicts three initial stages. The aim of this first snapshots is to show the early stages dynamics in which it is apparent that neurons receive the constant external current. After a while, a synchronization phenomenon arises, shown in Figure 4.4, followed by a travelling wave presented in Figure 4.5. Since there is no random connection external to a circle of radius 1/16 around each neuron, the framework is the same to those one seen in Figure 4.1 (b), with the exception of the choice of the initial datum.

Referring to the dynamics shown in Figures 4.3-4.4-4.5, the synchronization measure value is:

$$\chi = 0.4605 \ .$$

This quantity, less than 0.5, describes a low synchrony phenomenon in the network. Despite there is a synchronous excitatory phenomenon starting at $t = 30$, travelling waves then appear. Let us note that while $t > 60$, all the possible states are present in the network at the same time: the waves which travel in the whole domain determine which neurons are excited (ran over by the excitation), refractory (already been excited) or in a quiescent state (not yet excited). Thus, the high clustered connections are the responsible for strong differences in the membrane potential for each time. This translates into a low synchrony value.

4.2.2 Quasi-random connections

In order to reduce the topology regularity with respect to Section 4.2.1, new connections are introduced: we add to each neuron chemical synapses in the number of 2% of the total number of neurons in the network. Notably, for each cell i we choose additional chemically coupled neurons in the domain having distance greater than 1/16 from i. Neurons have equal probability to be chosen. In Figures 4.6-4.7-4.8, a sample dynamics is presented. It is worth noting that the excitation reaches wide areas of the network faster than in the previous case. Indeed, by comparing the frames on the right in

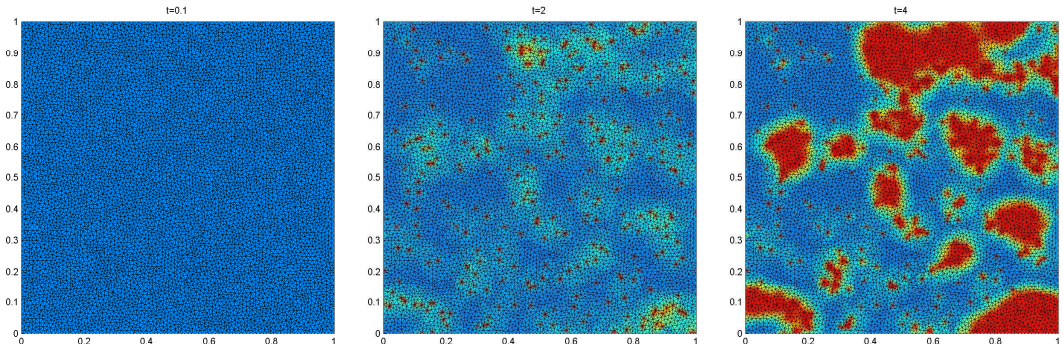

Figure 4.3: Early stage dynamics which involves 7933 neurons. For each cell, electrical synapses exist among nearest-neighbour neurons and the chemical ones are 75% of links among cells belonging to a circle having radius 1/16. The whole network is initially at rest but, after a while, a continuum external current $I = 0.1$ is applied to 319 of them randomly chosen. In the second frame, neurons which receive the injected current become apparent. In the third snapshot, a propagating phenomenon arises

Figures 4.3 and 4.6, the higher excitation degree of the second is apparent. From this consideration follows that a network with this kind of topology promotes wider excitation and synchronous excitation phenomena appear with high probability. In Figures 4.7-4.8, two events appear. The synchrony measure value, defined in (4.7), is:

$$\chi = 0.9368 \ .$$

This high value, near to one, numerically describes what can qualitatively be observed in the dynamics: for each time, the large majority of neurons are in the same state. This high value and the noticeable excitation phenomenon leads to the conclusion that when excitation arises, it involves wide network areas.

4.2.3 The effect of inhibitory neurons

The presence of inhibitory neurons is an important ingredient that should be dealt with. The aim of this paragraph is not to modify the topology, which is maintained unchanged from Section 4.2.2, but to throw in neurons which hinder the spread of excitation. Let us stress that, according to treatments in Paragraph 3.1, we characterize an inhibitory neuron with a negative reversal potential. Here, 20% of the neurons have a negative reversal potential: they inhibit all neurons reached through chemical synapses. Clearly, it is the value of the negative reversal potential which determines the inhibition size response. For this reason, two dynamics obtained with two different reversal potentials

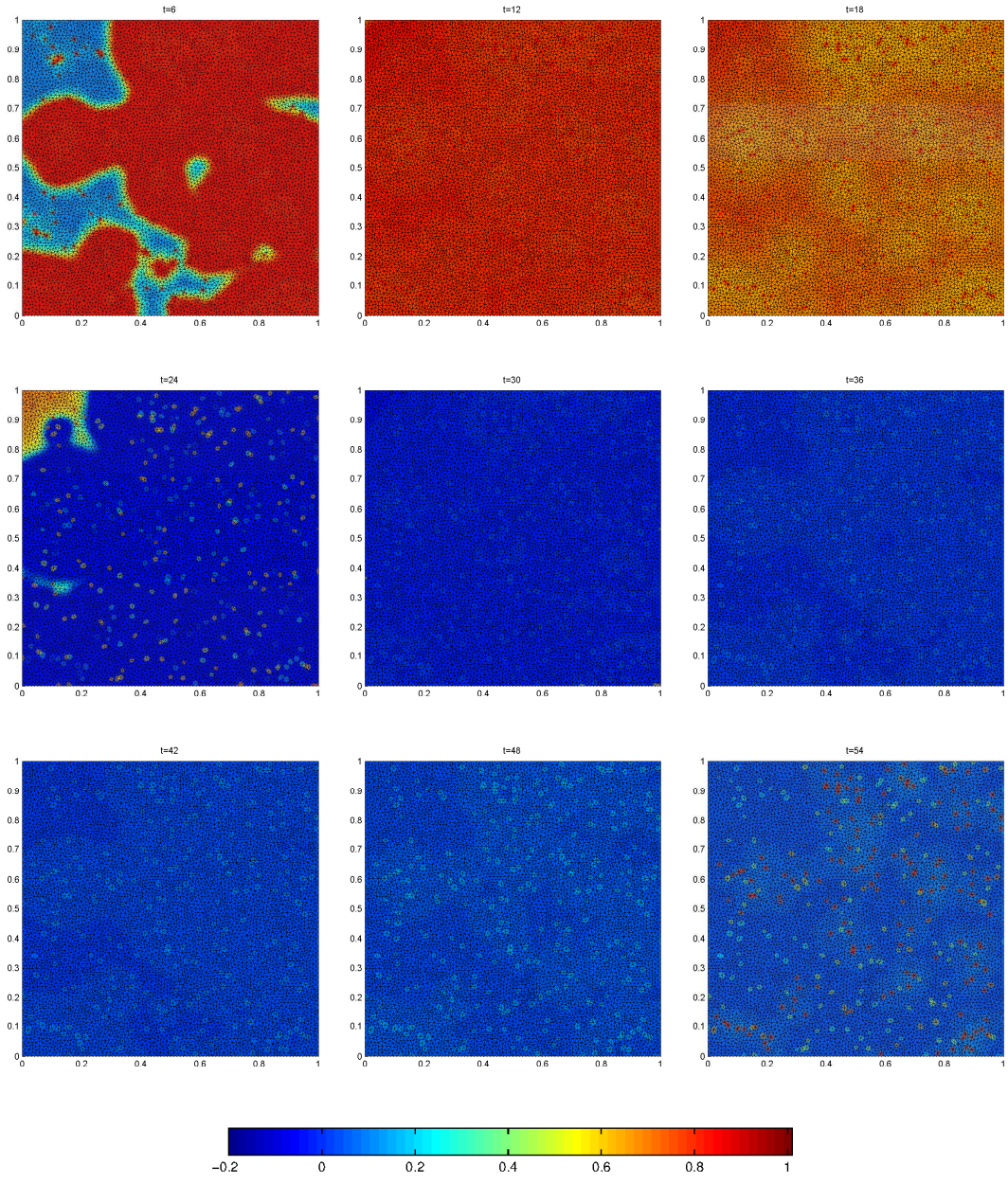

Figure 4.4: Course-time evolution of the early-stages dynamics shown in Figure 4.3. Notably, the synchronous excitation phenomenon is shown. After this, a completely different and asynchronous phenomenon arises, as depicted in Figure 4.5

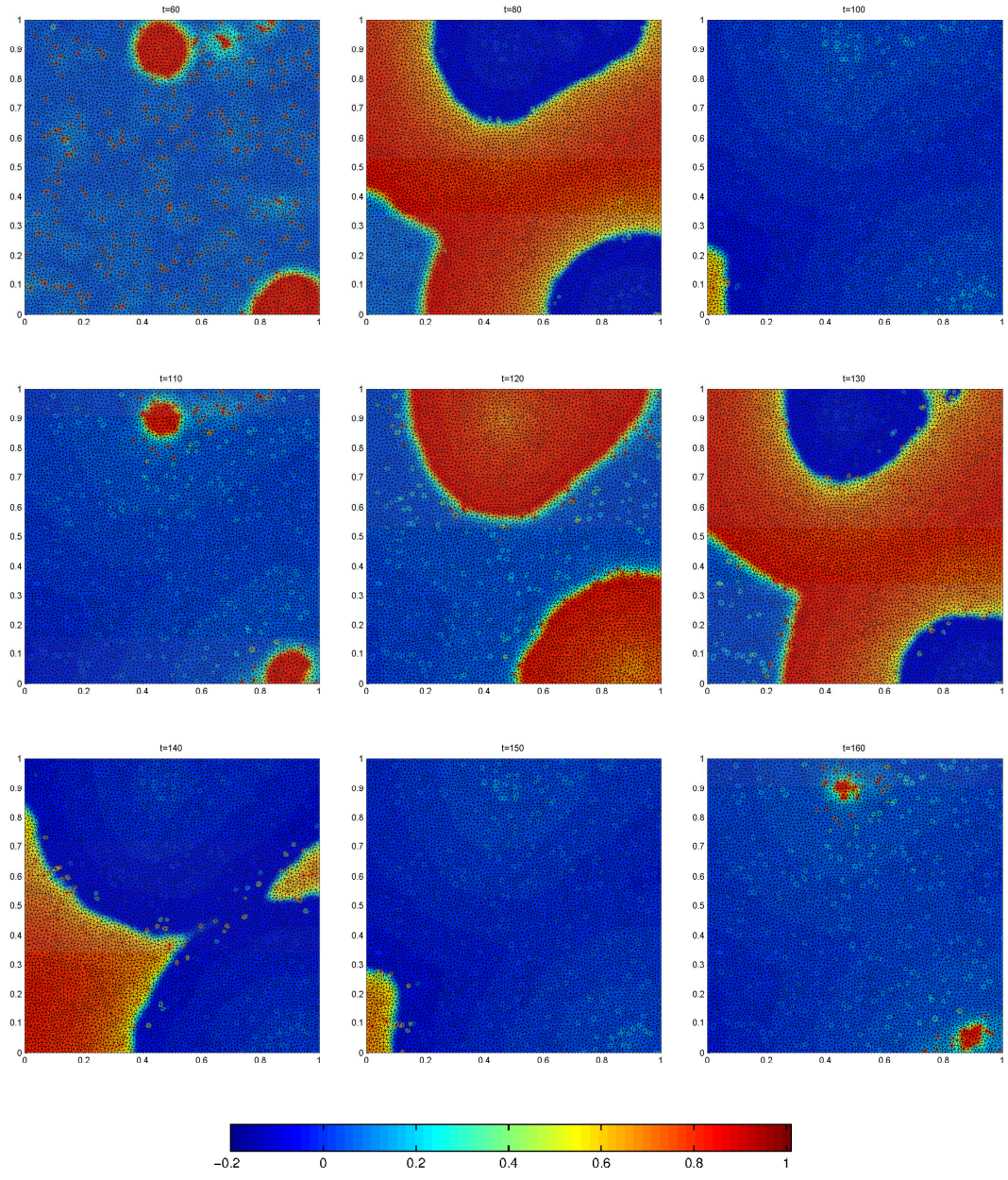

Figure 4.5: Last snapshots relative to the dynamics shown in Figures 4.3-4.4. A travelling wave arises from high clustered area. Since neurons enter in a stable limit cycle, they will continue to trigger the travelling wave

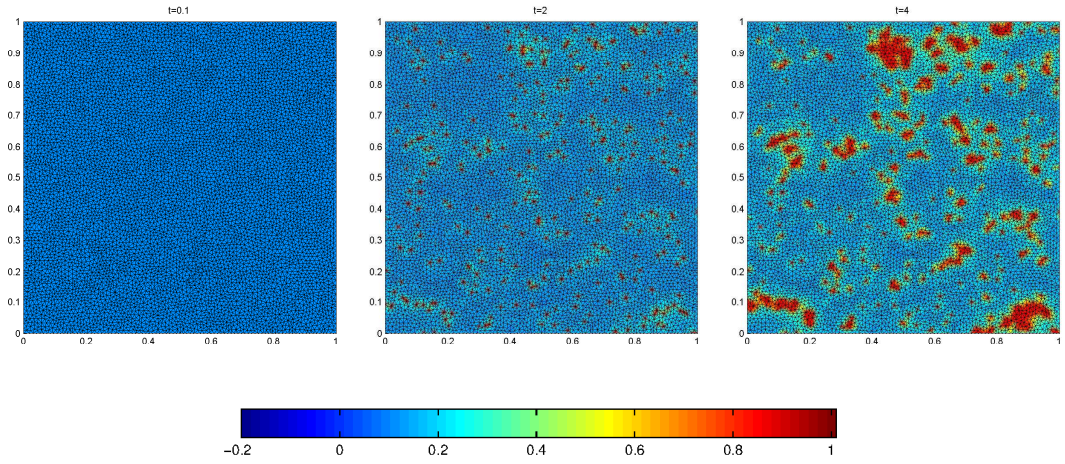

Figure 4.6: Early stage dynamics which involves 7933 neurons. For each cell, electrical synapses exist among nearest-neighbour neurons and the chemical ones are 75% of links among cells belonging to a circle having radius 1/16. The whole network is initially at rest but, after a while, a continuum external current $I = 0.1$ is applied to 319 of them randomly chosen. In the second frame, neurons which receive the injected current become apparent. In the third snapshot, a propagating phenomenon arises

are proposed. In the first case, the reversal potential for the randomly chosen inhibitory neurons is

$$v^I_{\rm syn} = -0.1 \ ,$$

while, in the second one

$$v^I_{\rm syn} = -0.9 \ .$$

The dynamics are shown in Figures 4.9-4.10-4.11 and Figures 4.12-4.13-4.14, respectively. The relevant consideration that comes from a qualitative analysis of these dynamics is that the presence of inhibition itself does not determine if excitatory synchronous event will appear. What decides this is the reversal potential value of the inhibitory neurons. Indeed, with a low $v^I_{\rm syn}$ value as in Figures 4.9-4.10-4.11, the inhibition does not preclude excitatory synchronous phenomena. On the contrary, these are excluded when an high $v^I_{\rm syn}$ value adversely influences the neuron responses. The quantitative measures are:

$$\chi = 0.9055 \quad \text{for} \quad v^I_{\rm syn} = -0.1 \ ,$$

and

$$\chi = 0.8089 \quad \text{for} \quad v^I_{\rm syn} = -0.9 \ .$$

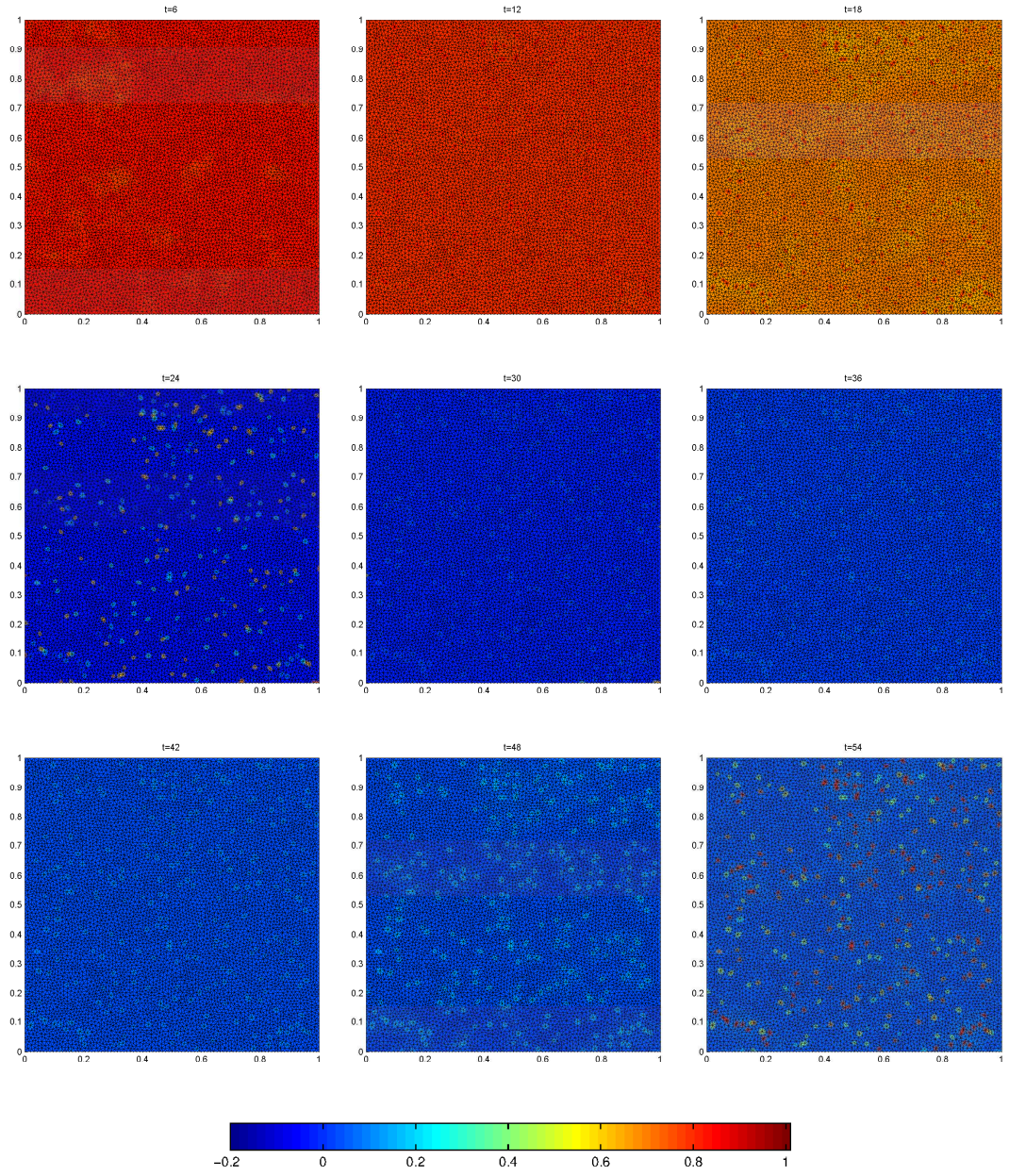

Figure 4.7: Snapshots following early stages dynamics in Figure 4.6. As well as in Figure 4.4, a synchronous phenomenon appears. The evolution of this dynamics is depicted in Figure 4.8.